



Published in final edited form as:

*J Nucl Cardiol.* 2019 June ; 26(3): 986–997. doi:10.1007/s12350-017-0942-8.

## An unmet clinical need: The history of thrombus imaging

Gregory M. Lanza, MD, PhD<sup>a</sup>, Grace Cui, MS<sup>a</sup>, Anne H. Schmieder, MS<sup>a</sup>, Huiying Zhang, MD<sup>a</sup>, John S. Allen, BS<sup>a</sup>, Michael J. Scott, BS<sup>a</sup>, Todd Williams, RT(R) MR<sup>a</sup>, and Xiaoxia Yang, BS<sup>a</sup>

<sup>a</sup>Department of Medicine, Division of Cardiology, Washington University Medical School, St. Louis, MO

### Abstract

Robust thrombus imaging is an unresolved clinical unmet need dating back to the mid 1970s. While early molecular imaging approaches began with nuclear SPECT imaging, contrast agents for virtually all biomedical imaging modalities have been demonstrated in vivo with unique strengths and common weaknesses. Two primary molecular imaging targets have been pursued for thrombus imaging: platelets and fibrin. Some common issues noted over 40 years ago persist today. Acute thrombus is readily imaged with all probes and modalities, but aged thrombus remains a challenge. Similarly, anti-coagulation continues to interfere with and often negate thrombus imaging efficacy, but heparin is clinically required in patients suspected of pulmonary embolism, deep venous thrombosis or coronary ruptured plaque prior to confirmatory diagnostic studies have been executed and interpreted. These fundamental issues can be overcome, but an innovative departure from the prior approaches will be needed.

### Keywords

Thrombus; fibrin; platelet; biomedical imaging

## INTRODUCTION

Effective thrombus formation is an essential facet of life required to maintain normal vascular hemostasis and to respond to injury whether accidental or surgical. Yet thrombosis can be the sine qua non of pathological events with serious or mortal consequence, such as acute myocardial infarction (AMI), deep venous thrombosis (DVT), pulmonary embolism (PE), or cerebral vascular arterial stroke (CVA). Indeed, fibrin deposits are the fertile matrix into which the neovasculature of cancers expand to fuel metastatic tumor progression. The pathological significance of thrombus has long been recognized and its specific diagnosis

Reprint requests: Gregory M. Lanza, MD, PhD, Division of Cardiology, Washington University Medical School, CORTEX building, Suite 101, 4320 Forest Park Ave, St. Louis, MO; greg.lanza@mac.com.

Electronic supplementary material: The online version of this article (doi:10.1007/s12350-017-0942-8) contains supplementary material, which is available to authorized users.

The authors of this article have provided a PowerPoint file, available for download at SpringerLink, which summarizes the contents of the paper and is free for re-use at meetings and presentations. Search for the article DOI on SpringerLink.com.

### Disclosure

The authors have no conflict to disclose.

led to contrast agent development efforts dating back to at least 1974. Although many targeted probes across a variety of imaging modalities have been proposed, no thrombus-specific diagnostics are commercially marketed within the US.

## THROMBOSIS: VASCULAR INFLAMMATION

Thrombosis is a complicated physiological process. Commonly, vessel wall injury triggers thrombus development, which involves the interplay of platelet activation and a cascade of enzymatic clotting proteins. Counter biochemical mechanisms by natural anti-coagulants and the fibrinolytic system modulate to prevent an over-exuberant progression. Thrombus formation is vascular inflammatory reaction wherein activated platelets adhere to the injured vessel wall and release cytokines, growth factors, and other pro-inflammatory mediators. Leukocytes, recruited to the site of vascular injury, adhere to P-selectin expressed on the activated platelet surface via P-selectin Glycoprotein Ligand-1 (PSGL-1).<sup>1</sup> Circulating microvesicles rich in tissue factor (TF) from leukocytes bind to platelet surface PSGL-1, sustaining the coagulation process triggered by vascular TF from endothelial injury.

Cross-communications between inflammation and coagulation biochemical networks are extensive. The local release of inflammatory cytokines induces leukocytes and endothelial cells to express TF.<sup>2</sup> Complexation of TF and the coagulation factor FVIIa or Xa incite coagulation on the negatively charged cell membranes. Thrombin, the major hemostatic coagulation enzyme, activates protease-activated receptors (PAR-receptors) highly expressed in platelets and endothelial cells, myocytes and neurons, which amplify the inflammatory pathway activity well beyond the acute coagulation process.<sup>3</sup> Fibrin, the mortar of clots, recruits and activates platelets through the platelet receptor  $\alpha_{IIb}\beta_3$ ,<sup>4</sup> as well as attracts leukocytes through interaction with the  $\alpha_M\beta_2$  (mac-1) integrin receptor.<sup>5</sup> Leukocyte binding to fibrin increases phagocytosis, NF $\kappa$ B-mediated transcription, production of chemokines and cytokines, and degranulation. Importantly, the inter-relationship between inflammation and coagulation in the pro-coagulant process also exists for the modulating anti-coagulant pathways centered around Tissue Factor Pathway Inhibitor (TFPI),<sup>6</sup> Antithrombin (AT),<sup>3</sup> Protein C/S.<sup>3</sup> The pro- and anti-coagulation and inflammatory pathways are counter balanced by endothelial cell responses to other physiological or pathological stimuli broadly including bacteria, toxins, trauma, and cytokines. While thrombus formation appears to be a simple process *en face*, it is, like other biological processes, a complicated and tightly regulated event.

## THROMBUS DIAGNOSTIC IMAGING

Despite the complexities of thrombus formation, medical imaging of the pathology has evolved with a more simplistic perspective based on the accumulation of fibrin or platelets. Both targets are richly present in both venous and arterial clots and offer the potential for bound contrast agents to provide requisite high contrast to blood/tissue signal for noninvasive imaging. Since the early 1970s, the development of thrombus-specific diagnostics has evolved along these two pathways with the earliest technologies being nuclear medicine approaches. Later, with expanding interest in molecular imaging, the most relevant modalities include ultrasound, magnetic resonance imaging (MRI), optical and

photoacoustic or optoacoustic imaging, and computed tomography (CT) including the newer Spectral or Multicolored CT.

### Fibrin Imaging

Fibrin is a major constituent of arterial and venous thrombi as well as thrombotic accretions to biomaterials such as stents, valves, wires, and other mechanical devices. Fibrinogen is a soluble, large, and complex 340 kDa glycoprotein that is converted by thrombin into fibrin during thrombus formation.<sup>7,8</sup> Synthesized by liver hepatocytes, fibrinogen circulates in plasma at levels between 200 and 400 mg/dL. During normal blood coagulation, prothrombin is converted into thrombin, a serine protease, which subsequently converts soluble fibrinogen into insoluble fibrin strands. These insoluble fibrin fibrils become further cross-linked strands by circulation clotting factor XIIIa (FXIIIa) to yield a stabilized clot.<sup>9</sup> Beyond cross-linking, FXIIIa further stabilizes the fibrin clots by entrapment of fibrinolysis inhibitors alpha-2-antiplasmin<sup>10</sup> and TAFI (thrombin activatable fibrinolysis inhibitor, procarboxypeptidase B),<sup>11</sup> and by interacting with cell adhesive receptors presented by inflammatory cells. Activated coagulation factors such as Factor Xa and thrombin also bind to fibrin and become transiently inactivated by entrapment within the fibrin fibril network. Fibrin simultaneously triggers the pro-coagulant pathway via activation of factor XIII by thrombin and the anti-coagulant pathway through plasminogen activator, such as tissue plasminogen activators (TPA).<sup>12</sup>

Early probes sought to label and incorporate natural constituents of clot formation, the first one being <sup>125</sup>I radiolabeled fibrinogen.<sup>13–15</sup> This gamma nuclear probe produced promising increases in detection results relative to negative controls, but the data were only loosely correlated with thrombus fibrin content; imaging was delayed 24 to 72 hours, and after clot lysis significant intramural nuclear signal remained in the vessel walls creating frequent false positive interpretations. Shortly after the first <sup>125</sup>I fibrinogen probes, the development of <sup>111</sup>In-platelets was pursued creating the second general pathway to thrombus detection.<sup>16</sup> In overview, this approach dominated investigator interest for a decade. However, around this time Niels Jerne's earlier theories concerning the specificity in development and control of the immune system<sup>17,18</sup> were combined with the discovery of the principles for production monoclonal antibodies by Köhler and Milstein.<sup>19</sup> These discoveries and investigators were recognized with a shared Nobel Prize for Physiology or Medicine in 1984<sup>20</sup> and presented the opportunity to pursue dedicated antibodies specific for fibrin and later platelets.

Before the wider availability of monoclonal antibodies, <sup>131</sup>I anti-fibrin rabbit polyclonal antibodies were studied in patients with thrombophlebitis or chronic varicosities. The new technique detected formed or developing clots and helped to discriminate between thrombophlebitis, best detected 24 to 72 hours post-injection, and thrombus-free varices, discerned optimally after 6 hours.<sup>21</sup> Ten years later, Grossman et al reported thrombus imaging with <sup>111</sup>In-labeled anti-fibrin monoclonal antibodies and F<sub>(ab)</sub>2 fragments.<sup>22</sup> They achieved better CNR using the more rapid clearing F<sub>(ab)</sub>2 probes than the more circulatory persistent antibodies. Subsequently, the question of fibrin vs platelet imaging was addressed for the first of several times with <sup>131</sup>I-anti-fibrin antibodies injected simultaneously

with  $^{111}\text{In}$ -platelets.<sup>23</sup> The anti-fibrin approach demonstrated 60% higher clot uptake vs the  $^{111}\text{In}$ -platelets reference.<sup>23</sup> Similarly, comparisons between murine monoclonal antibody  $^{125}\text{I}$   $\text{F}_{(\text{ab})}$  and  $\text{F}_{(\text{ab})2}$  fragments were performed to determine the optimal balance between maximum thrombus binding and rapid blood pool clearance in rabbits and not unexpectedly the higher avidity  $\text{F}_{(\text{ab})2}$  fragment proved superior to  $\text{F}_{(\text{ab})}$ .<sup>24</sup>

However, given the close relationships between fibrinogen and fibrin, efforts to produce ligands with higher fibrin specificity were pursued. The best monoclonal antibody candidates created in this quest were developed by Patrick Gaffney at the National Institute of Biological Standards and Controls (NIBSC) in London<sup>25–28</sup> and by Bohdan Kudryk at the New York Blood Center.<sup>29–32</sup> While these monoclonal antibodies were used in several subsequent molecular imaging studies with multiple modalities discussed subsequently, neither fibrin ligand achieved clinical translation.

Another highly specific family of monoclonal antibodies were raised to D-dimer, a site formed when adjacent fibrin D-domains cross-link.<sup>31</sup> This neo-epitope and its degradation product were not present in monomeric fibrin fibrils or fibrinogen and immunoscintigraphy and biodistribution studies in rats confirmed high thrombus specificity with little normal tissue background for this probe. Subsequent preclinical and eventual clinical studies were conducted with  $\text{F}_{(\text{ab})}$  fragments of this antibody, most notably DD/3B6, but the probe never became clinically established.<sup>33–35</sup> One challenge for the DD/3B6 target was its spontaneous liberation from the clot into blood, which variably reduced the thrombus retained antigen and concurrently generated circulating D-dimer that could potentially interfere with targeted imaging. Today D-dimer assays in blood are routinely used to exclude thrombotic disease, such as pulmonary embolus or deep venous thrombosis.<sup>36</sup>

Developments in phage display recombinant peptide panning and selection led to the discovery and use of smaller molecular weight fibrin binding peptides.<sup>37</sup> For fibrin targeting, the most effective probes were identified and developed by Epix Pharmaceuticals of Cambridge, MA. Epix had produced an MRI contrast Gadofosveset trisodium, which spontaneously coupled with circulating albumin to increase relaxivity and lengthen blood pool contrast persistence. A complicated and evolving set of corporate arrangements with Mallinckrodt Chemical Co, Siemens, Schering, Berlex, and lastly Lantheus Medical Imaging, led to product launch in the US and then worldwide as ABLAVAR<sup>®</sup> in 2010. During this timeframe, Epix Pharmaceutical became interested in the development of a fibrin paramagnetic MR molecular imaging probe based on the coupling of chelated gadolinium, typically 4 Gd-DOTA per peptide<sup>38</sup> and applied their MR contrast development expertise to this goal. Epix developed families of well-characterized fibrin-binding peptides,<sup>39</sup> which were extensively tested in the preclinical<sup>40–47</sup> and later clinical setting.<sup>48</sup> Yet, despite the strength of this seminal product concept, the technology failed to reach the market and clinical use.

Another commercial approach included Tc-NC100668, a peptide partial analogue mimic of  $\alpha_2$ -antiplasmin.<sup>49–51</sup> Uniquely, this ligand was effective for targeting venous thrombosis in the presence of anticoagulants and thrombolytics, which led others to later adopt this homing strategy.

## Platelet Imaging

While radiolabeled fibrinogen imaging initiated the quest to develop thrombus-specific imaging agents, this approach was quickly superseded by  $^{111}\text{In}$ -labeled platelet imaging.<sup>16,52</sup> Both radiolabeled fibrinogen and platelets in patients showed relatively low signal initially but platelet imaging had modestly better results with acute clots less than 24 hours.<sup>53</sup> Retrospectively this finding was prescient and points to a key limitation impacting most published thrombus imaging probes to date. The inadequate uptake of  $^{111}\text{In}$  platelets by aged thrombus compared with acute thrombus was further validated in canines.<sup>54</sup> Since common clinical practice for patients suspected of DVT or PE dictates anti-coagulation until the diagnoses are ruled out, Fedullo et al assessed the impact of heparin on  $^{111}\text{In}$  platelet imaging.<sup>55</sup> Their experiment in dogs demonstrated that heparin anti-coagulation markedly inhibited  $^{111}\text{In}$  platelet uptake until its effects were reversed by protamine.<sup>55</sup> This was another prophetic result,<sup>56</sup> which continues to haunt the development and translation of thrombus imaging agents. Despite these limitations,  $^{111}\text{In}$  platelet imaging research continued robustly for a decade in the context of LV thrombus,<sup>57–60</sup> acute cerebrovascular thrombosis,<sup>61</sup> iliac arterial mural thrombosis,<sup>62</sup> and DVT.<sup>63</sup>

The use of radiolabeled platelets gave way to platelet binding ligands that were adopted to circumvent issues with limited platelet uptake in aged clot and during anti-coagulation, to overcome the inconvenience of harvesting, washing, and labeling of patient platelets for study, and to accelerate image acquisition following treatment. In 1985, initial results with anti-platelet (anti-GPIIb/IIIa) monoclonal antibodies (7E3) were reported in vitro and in dogs.<sup>64</sup> Again, acute thrombus could be imaged but 48h thrombus was not detectable. Another monoclonal antibody (SZ-51) was developed against a platelet epitope, alpha granule membrane protein (GMP-140), which was later characterized to be P-selectin.  $^{65-131}\text{I}$ -SZ-51 was initially shown to be effective against acute dog thrombus<sup>66</sup> and was later modified into a mouse-human chimeric ligand that was characterized in vitro.<sup>65,67</sup> However, both monoclonal approaches failed to progress significantly. In parallel with the events in fibrin targeting, platelet homing ligands targeting the GP IIb/IIIa receptor took many forms over the years including: radiolabeled small molecule receptor antagonists,<sup>68–70</sup> disintegrins,<sup>71–73</sup> and peptides.<sup>74–78</sup> Unfortunately, none have translated to the clinic.

## ALTERNATIVE MODALITIES FOR MOLECULAR IMAGING OF THROMBUS

Gamma emitter-based nuclear imaging approaches dominated thrombus imaging from the mid-70s into the mid-90s. Beginning in the mid-90s, thrombus contrast agent development for alternative imaging modalities emerged involving nanoparticles, microbubbles, optical, and PET.

### Ultrasound

The first ultrasound contrast agent for thrombus was demonstrated in dogs in 1996 (Figure 1). This ligand-targeted nanoparticle utilized perfluorocarbon (PFC) emulsions, which offered negligible acoustic contrast in circulation at low doses, but nanoparticle binding to arterial thrombus generated enhanced acoustic reflectivity.<sup>79</sup> One can imagine the PFC particles acting like silver grains accumulating on a glass plate to create a mirror.<sup>79–81</sup> The

echogenicity of clot bound PFC nanoparticles was easily appreciated within 30 to 60 minutes because the blood pool background signal was negligible. This was in stark contrast to the high background noise of nuclear approaches that could delay immunoscintigraphic imaging for days. Continued research by Hughes et al developed new and improved acoustic detection approach based on entropy detection that optimized ultrasonic PFC molecular imaging. Entropy imaging is a statistical spatial and temporal index wherein the reflected RF signal variation in each ultrasound line of data is projected as a histogram and the characteristics of the histogram are mapped as an image as opposed to the common approach of using reflected RF power.<sup>82-86</sup> While these experimental approaches to ultrasound imaging offered significant advancements in general, the fundamental techniques used by echocardiographic equipment better complemented microbubble use, which was gaining effectiveness for blood pool imaging of the heart and later molecular imaging as discussed below.

In 1999, echogenic liposomes (ELIP), which had been reported as an early concept for acoustic thrombus imaging,<sup>87,88</sup> were demonstrated in vivo for intravascular clots.<sup>89</sup> These submicron liposomal particles were developed to avoid the transpulmonary particle entrapment issues experienced by microbubbles being developed for intracardiac blood pool imaging in the early 1990s. While the acoustic reflectivity of ELIP was less than microbubbles and circulatory stability less than perfluorocarbon nanoparticles, ELIP particles have found therapeutic applications involving intravascular gas and thrombolytic delivery.<sup>90-94</sup>

In 2002, microbubble development by ImaRx Therapeutics, which invented, developed and licensed Definity<sup>®</sup> microbubbles for cardiac imaging, reported modification of their bubbles to target platelet GP IIb/IIIa receptors in vitro. Later, the company developed abciximab-targeted microbubbles, which targeted the GP IIb/IIIa receptors on platelets, and demonstrated the formulation in vitro and in rats with carotid occlusions.<sup>95</sup> ImaRx continued to pursue microbubble-based thrombus imaging and compared fibrin- and platelet-directed bubbles in vitro concluding that fibrin-targeted microbubbles produced greater signal.<sup>96</sup> This outcome was reminiscent of the conclusion previously advanced by Bosnjakovic et al comparing <sup>111</sup>In platelets with <sup>131</sup>I anti-fibrin antibodies.<sup>23</sup> Wang et al targeted GP IIb/IIIa platelet receptor with a single-chain antibody-microbubble construct, which was shown to target thrombus and provide imaging confirmation of thrombolysis.<sup>97</sup> During the same time period, Hu et al reported and RGD-peptide-microbubble agent studied its binding under varying shear conditions, and demonstrated enhanced acoustic contrast against aortic thrombus compared with control microbubbles.<sup>98,99</sup> In addition to imaging, microbubbles offer a theranostic component to the treatment of thrombus through mechanical disruption by particle cavitation and local release of fibrinolytic agents.<sup>100,101</sup>

### Magnetic Resonance Imaging

Thrombus-specific MR imaging was first reported in 1998 using fibrin-specific monoclonal antibodies produced by Patrick Gaffney at the NIBSC to target paramagnetic perfluorocarbon nanoparticles, as previously used for acoustic thrombus imaging.<sup>102</sup> The lipid-encapsulated PFC particles incorporated lipid-anchored Gd-DTPA at high payloads



that markedly increased the ionic (Gd-based) and particulate (NP-based) relaxivity and overcame partial volume signal dilution (Figure 2).<sup>102</sup> Further development of these nanoparticles for thrombus imaging optimized Gd-chelate loading and the relative particle surface positioning of the metal.<sup>103</sup> In the mid-2000s, further imaging and gadolinium stability optimization with these particles were achieved with the use of Gd-DOTA prior to Australian clinical trials. Unexpectedly, these Phase I clinical studies were paused then eventually discontinued when some early patients complained of transient back pain occurring at very low contrast dosages of the imaging agent. Despite extensive safety testing in vitro and in mice, rats, rabbits, dogs, and baboons without adverse complications, recognition of this issue was only triggered late by patient comments. The problem was identified as acute complement activation and was extensively characterized.<sup>104</sup> Subsequent advancements in clinical <sup>19</sup>fluorine imaging spurred a return of this technology without gadolinium to the clinic in the context of angiogenesis MR molecular imaging.

A similar perfluorocarbon particle targeted to thrombus in the IVC of mice via an  $\alpha_2$ -antiplasmin peptide was imaged successfully using high-field <sup>19</sup>F MRI (9.4T).<sup>105</sup> The results corroborated the thrombus <sup>1</sup>H imaging earlier in dogs in 1998<sup>102</sup> and later in vitro and then in vivo during 2000 to 2001<sup>106,107</sup> with 4.7T and clinical 1.5T scanners, respectively. As previously mentioned, the first of many reports involving the Epix paramagnetic peptides agent reached the scientific literature in 2004, representing the first modern MR thrombus imaging program to reach Phase II clinical studies.<sup>40</sup>

In 2001, working with Nycomed (Norway), Johansson reported the first platelet-targeted MR approach using ex vivo and in vivo models based on an RGD-USPIO probe (ultrasmall superparamagnetic iron oxide).<sup>108</sup> Subsequently in 2008, MPIO (microparticles of iron oxide) targeted with single-chain antibodies directed to platelet GP IIb/IIIa in mice were reported.<sup>109</sup> The thrust of using large iron oxide particles was to improve contrast but importantly take advantage of rapid macrophage phagocytic system clearance of the large particles in order to shorten the time from injection to MR imaging, overcoming the 24 to 72 hours delays typically required before imaging long circulating USPIO particles.

Recently, a new form of MR-related tomographic imaging was developed and studied known as Magnetic Particle imaging.<sup>110</sup> MPI varies from MRI by utilizing changing magnetic fields to produce a single magnetic field free region. Using shape optimized SPIO (superparamagnetic iron oxide) nanoparticles, signal is generated only in this region, which is moved systematically to produce an image that avoids the interfering iron contrast background that delays post-injection image acquisition. The MPI molecular imaging concept was tested in 2013 using a fibrin-peptide functionalized SPIO in vitro to produce about 200 times more signal than traditional MR magnetic particle spectroscopy.<sup>111</sup> This unique opportunity for ultrahigh MR molecular imaging sensitivity is very attractive, but both the instrumentation and iron oxide contrast development need to progress much further.

The versatility of MR imaging can be used to exploit the inherent MR magnetic properties of thrombus using techniques like magnetization transfer (MT) and diffusion imaging (DI) techniques.<sup>112</sup> Serial imaging of IVC thrombus in mice demonstrated that older densely organized thrombus, which is typically resistant to fibrinolytic therapy, was visualized well

with MT signal and poorly with DI. For younger lytic responsive thrombus, the converse was noted: high DI efficacy but low MT signal.

Some investigators have pursued other clever targeting approaches to thrombus, such as Myerson et al who used an irreversible thrombin inhibitor (PPACK) to bind thrombin on carotid clots in vivo for MR imaging of PFC particles.<sup>113</sup> These results further suggested a theranostic potential to the construct, which also interfered with continued thrombus progression.

### Computed Tomography

The bromine atom associated with each molecule of perfluorooctyl bromide used in some PFC nanoparticles inherently provides CT contrast. The accumulation of fibrin-targeted nanoparticles on clots can impart significant x-ray opacity to thrombus.<sup>114</sup> In this regard, PFC nanoparticles offer multi-multimodal-targeted contrast consistent with early blood pool observations by Mattrey in the early 1980s.<sup>115–117</sup>

CT imaging has made many advances in both detector hardware and software reconstruction. Perhaps one of the newest and most exciting involves Spectral or Multicolor CT based on K-edge imaging.<sup>118</sup> Every element has electrons that inhabit energy “shells” which surround the nucleus. The shell closest to the nucleus is designated the K-shell. K-edge imaging exploits an absorption discontinuity created when an emitted x-ray photon with energy identical to or larger than the energy of the K-shell electron fuse. An abrupt rise in attenuation at that energy is noted within the x-ray spectrum, the K-edge. CT scanners with K-edge imaging capability can be engineered with different hardware x-ray tube and detector configurations; one advanced system uses a standard x-ray tube and a new multilayered photon counting detector that counts and characterizes the energy of each photon striking it. These clinical instruments utilize advanced reconstruction techniques to calculate and deconvolve three types of x-ray energy on a voxel by voxel basis: Compton, photoelectric, and K-edge data. The Compton and photoelectric energies are used to create the standard x-ray CT image on which the K-edge data can be superimposed without registration issues because all the data are derived simultaneously. Molecular imaging contrast agents for CT, particularly Spectral CT, can be achieved by incorporating sufficient metal loads of elements ranging from iodine to bismuth on the periodic table into nanoparticles. The K-shell electron energies of these elements correspond to the photon energies emitted by a typical x-ray tube. The first example of fibrin imaging with a Spectral CT contrast agent and scanner was reported by Pan et al based on bismuth organometallic complexes and demonstrated in vitro and in femoral-iliac thrombus in rabbits (Figure 3).<sup>119</sup> This was followed by studies with Spectral CT particles based on ytterbium organo-complexes or minute gold nanoparticles suspended in “oil” and encapsulated with phospholipids.<sup>120–122</sup> Although not specifically addressing fibrin imaging, Cormode et al have spent considerable energy developing contrast agents for Spectral CT imaging.<sup>123–126</sup> For thrombus imaging, the potential of Spectral CT rests in its development of speed of acquisition, which 1-day could reach a level to permit ruptured plaque imaging in coronary beds and pulmonary embolus imaging.



## Optical-Related Imaging

In 2004, Jaffer et al reported a near-infrared (NIR) optical imaging approach to thrombus detection and characterization conducted in vitro and in rats that utilized a peptide homing to Factor XIIIa.<sup>127</sup> Jaffer utilized Factor XIIIa as an acute thrombus marker with the potential to assess thromboembolic risk and susceptibility to fibrinolysis. The next year, this team demonstrated the development of a fluorescent probe targeted via a branched peptide against platelet GP IIb/IIIa.<sup>77</sup> The lab continued development of optical probes using one of the Epix Pharmaceutical fibrin binding peptides conjugated to a Cy7 NIR dye-to detect acute DVT in rats.<sup>128</sup> Like the use of Factor XIIIa targeting this probe could stratify venous thromboembolism for fibrinolysis.<sup>129</sup>

Photoacoustics or optoacoustics invoke the use of endogenous proteins, cells, or contrast agents to adsorb gated laser light pulses to create minute levels of heat (nanojoules) that dissipates the energy as acoustic emissions. These emissions are detectable with standard single element or even clinical ultrasound transducers. As an example, gold nanobeacons (GNB) incorporate a multitude of tiny (4 to 5 nm) gold nanoparticles into an oil suspension and target thrombus using fibrin antibodies in vitro.<sup>130</sup> The dense incorporation of gold particles within the lipid-encapsulated particles generated a very strong photoacoustic signal effectively similar to a much larger gold particle. However, because the human renal clearance threshold for particles is about 8 nm, larger non-degradable particles will be retained in the body indefinitely, potentially posing future safety issues, while particles below this size will be eliminated in urine. As opposed to technologies where local injection of gold particles limits treatment cost, systemic therapies for thrombus detection will require orders of magnitude more gold and increase treatment cost substantially. To address this issue, high-density organometallic suspensions of divalent copper in lipid-encapsulated nanoparticles were developed for fibrin imaging with MRI<sup>131</sup> and then used for systemic photoacoustic imaging and anti-angiogenic drug delivery (fumagillin prodrug) targeted to the sparse  $\alpha v \beta 3$ -integrin receptor expressed by nascent neovessel sprouts.<sup>132</sup> These copper-rich nanoparticles demonstrated NIR photoacoustic reflectivity similar to gold GNB.

## Positron Emission Tomography

While the vast abundance of early nuclear medicine probes for fibrin or platelet imaging involved gamma emitters, such as <sup>99m</sup>Tc, <sup>125</sup>I, <sup>131</sup>I, or <sup>111</sup>In, recent PET probes based on <sup>64</sup>Cu<sup>133</sup> have been reported for thrombus imaging. These investigators described one peptide, called FBP8, as an effective fibrin-specific probe, originally described within the Epix Pharmaceutical IP estate, but its efficacy was greatest towards acute thrombus and diminished quickly as the clot aged. The loss of thrombus binding paralleled a reduction in fibrin content as the clots organized.<sup>134,135</sup>

## SUMMARY

Thrombus imaging has a rich history dating back to the mid 1970s and continuing to the present. This continued effort is fueled by an unresolved clinical unmet need, perhaps greatest for pulmonary embolism, ischemia-reperfusion injury microthrombus, and unstable ruptured or eroded carotid and coronary atherosclerotic plaques. While early molecular

imaging approaches began with nuclear SPECT imaging, contrast agents for virtually all biomedical imaging modalities have been reported, each offering some unique strengths and weaknesses. Despite years of study, platelets and fibrin remain the dominant thrombus targets. Acute thrombus is readily imaged with all probes, but aged thrombus remains difficult to target. Similarly, anti-coagulation continues to interfere and often negate thrombus imaging probe efficacy, yet the use of this therapy is clinically demanded when pulmonary embolism, DVT or coronary ruptured plaques are suspected. The lack of a clinical thrombus imaging contrast agent reflects the difficulty of overcoming these fundamental challenges that will require an “out of the box” design approach.

## Supplementary Material

Refer to Web version on PubMed Central for supplementary material.

## Acknowledgments

**Funding:** This review was supported in whole or part by Grants from the CA199092 (G.M.L.) CA154737 (G.M.L.), HL122471 (G.M.L.), HL112518 (G.M.L.), HL113392 (G.M.L.), HHSN26820140042C (G.M.L.), and HL112518 (G.M.L.)

## References

1. Furie B, Furie BC. Role of platelet P-selectin and microparticle PSGL-1 in thrombus formation. *Trend Mol Med*. 2004; 10:171–8.
2. Foley JH, Conway EM. Cross talk pathways between coagulation and inflammation. *Circ Res*. 2016; 118:1392–408. [PubMed: 27126649]
3. High KA. Antithrombin III, protein C, and protein S. Naturally occurring anticoagulant proteins. *Arch Pathol Lab Med*. 1988; 112:28–36. [PubMed: 2962557]
4. Litvinov RI, Farrell DH, Weisel JW, Bennett JS. The platelet integrin alpha IIb beta 3 differentially interacts with fibrin versus fibrinogen. *J Biol Chem*. 2016; 291:7858–67. [PubMed: 26867579]
5. Podolnikova NP, Podolnikov AV, Haas TA, Lishko VK, Ugarova TP. Ligand recognition specificity of leukocyte integrin alpha M beta 2 (Mac-1, CD11b/CD18) and its functional consequences. *Biochemistry*. 2015; 54:1408–20. [PubMed: 25613106]
6. Wood JP, Ellery PE, Maroney SA, Mast AE. Biology of tissue factor pathway inhibitor. *Blood*. 2014; 123:2934–43. [PubMed: 24620349]
7. Scheraga H, Laskowski M Jr. The fibrinogen-fibrin conversion. *Adv Protein Chem*. 1957; 12:1–131.
8. Waugh DF. Protein-protein interactions. *Adv Protein Chem*. 1954; 9:325–437. [PubMed: 13217921]
9. Selmayr E, Mahn I, Muller-Berghaus G. Crosslinking of soluble fibrin and fibrinogen. *Thromb Res*. 1985; 39:467–74. [PubMed: 2864751]
10. Fraser SR, Booth NA, Mutch NJ. The antifibrinolytic function of factor XIII is exclusively expressed through alpha(2)-antiplasmin cross-linking. *Blood*. 2011; 117:6371–4. [PubMed: 21471521]
11. Walker JB, Bajzar L. The intrinsic threshold of the fibrinolytic system is modulated by basic carboxypeptidases, but the magnitude of the antifibrinolytic effect of activated thrombin-activable fibrinolysis inhibitor is masked by its instability. *J Biol Chem*. 2004; 279:27896–904. [PubMed: 15128744]
12. Camiolo SM, Thorsen S, Astrup T. Fibrinogenolysis and fibrinolysis with tissue plasminogen activator, urokinase, streptokinase-activated human globulin, and plasmin. *Proc Soc Exp Biol Med*. 1971; 138:277–80. [PubMed: 5125527]
13. O'Brien JR. Detection of thrombosis with iodine-125 fibrinogen. *Lancet*. 1970; 296:396–8.
14. Kerrigan GNW, Buchanan MR, Cade JF, Regoeczi E, Hirsh J. Investigation of the mechanism of false positive <sup>125</sup>I labelled fibrinogen scans. *Br J Haematol*. 1974; 26:469–73. [PubMed: 4852563]

15. Hirsh J, Gallus AS. <sup>125</sup>I-labeled fibrinogen scanning: use in the diagnosis of venous thrombosis. *JAMA*. 1975; 233:970–3. [PubMed: 125351]
16. Thakur ML, Welch MJ, Joist JH, Coleman RE. Indium-111 labeled platelets: studies on preparation and evaluation of in vitro and in vivo functions. *Thromb Res*. 1976; 9:345–57. [PubMed: 824756]
17. Jerne NK. The natural-selection theory of antibody formation. *Proc Natl Acad Sci USA*. 1955; 41:849–57. [PubMed: 16589759]
18. Jerne NK, Nordin AA. Plaque formation in agar by single antibody producing cells. *Science*. 1963; 140:405.
19. Köhler G, Milstein C. Continuous cultures of fused cells secreting antibodies of predefined specificity. *Nature*. 1975; 256:495–7. [PubMed: 1172191]
20. Alkan SS. Monoclonal antibodies: the story of a discovery that revolutionized science and medicine. *Nat Rev Immunol*. 2004; 4:153–6. [PubMed: 15040588]
21. Bosnjakovic VB, Jankovic BD, Horvat J, Cvoric J. Radiolabelled anti human fibrin antibody: A new thrombus detecting agent. *Lancet*. 1977; 1:452–4. [PubMed: 65564]
22. Grossman ZD, Rosebrough SF, McAfee JG, Subramanian G, Ritter-Hrncirik CA, Witanowski LS, et al. Imaging fresh venous thrombi in the dog with I-131 and In-111 labeled fibrin-specific monoclonal antibody and F(ab')<sub>2</sub> fragments. *Radiographics*. 1987; 7:913–21. [PubMed: 3454034]
23. Bosnjakovic V, Jankovic BD, Horvat J, Nastic-Miric D, Djukic V, Pavlovic S. The validity of radiolabeled anti fibrin antibody for deep vein thrombosis imaging. *Eur J Nucl Med Mol Imaging*. 1988; 14:489–94.
24. Hashimoto Y, Stassen JM, Leclef B, De Roo M, Vandecruys A, Melin J, et al. Thrombus imaging with an I-123-labeled F(ab')<sub>2</sub> fragment of an anti-human fibrin monoclonal antibody in a rabbit model. *Radiology*. 1989; 171:223–6. [PubMed: 2928528]
25. Edgell T, McEnvoy F, Webbon P, Gaffney P. Monoclonal antibodies to human fibrin: Interaction with other animal fibrins. *Thromb Haemost*. 1996; 75:595–9. [PubMed: 8743185]
26. Tymkewycz PM, Creighton Kempford LJ, Gaffney PJ. Generation and partial characterization of five monoclonal antibodies with high affinities for fibrin. *Blood Coagul Fibrinolysis*. 1993; 4:211–21. [PubMed: 7684615]
27. Tymkewycz PM, Creighton Kempford LJ, Hockley D, Gaffney PJ. Screen for fibrin specific monoclonal antibodies: the development of a new procedure. *Thromb Haemost*. 1992; 68:48–53. [PubMed: 1514172]
28. Tymkewycz PM, Creighton LJ, Gascoine PS, Zanelli GD, Webbon PM, Gaffney PJ. Imaging of human thrombi in the rabbit jugular vein: I: Comparison of two fibrin-specific monoclonal antibodies. *Thromb Res*. 1989; 54:411–21. [PubMed: 2772866]
29. Kudryk BJ, Bini A, Kumar SR, Zlokovic BV. Monoclonal antibody designated T2G1 reacts with human fibrin β-chain but not with the corresponding chain from mouse fibrin. *Arterioscler Thromb Vasc Biol*. 2000; 20:1848–9. [PubMed: 10894828]
30. Rosebrough S, McAfee J, Grossman Z, Kudryk B, Ritter-Hrncirik C, Witanowski L, et al. Thrombus imaging: A comparison of radiolabeled GC4 and T2G1s fibrin-specific monoclonal antibodies. *J Nucl Med*. 1990; 31:1048–54. [PubMed: 2348234]
31. Rosebrough SF, Grossman ZD, McAfee JG, Kudryk BJ, Subramanian G, Ritter-Hrncirik CA, et al. Thrombus imaging with indium-111 and iodine-131-labeled fibrin-specific monoclonal antibody and its F(ab')<sub>2</sub> and Fab fragments. *J Nucl Med*. 1988; 29:1212–22. [PubMed: 3392581]
32. Kudryk B, Rohoza A, Ahadi M, Chin J, Wiebe ME. Specificity of a monoclonal antibody for the NH<sub>2</sub>-terminal region of fibrin. *Mol Immunol*. 1984; 21:89–94. [PubMed: 6200769]
33. Macfarlane DJ, Smart RC, Tsui WW, Gerometta M, Eisenberg PR, Scott AM. Safety, pharmacokinetic and dosimetry evaluation of the proposed thrombus imaging agent <sup>99m</sup>Tc-DI-DD-3B6/22-80B3 Fab'. *Eur J Nucl Med Mol Imaging*. 2006; 33:648–56. [PubMed: 16528525]
34. Macfarlane D, Socrates A, Eisenberg P, Larcos G, Roach P, Gerometta M, et al. Imaging of deep venous thrombosis in patients using a radiolabelled anti-D-dimer Fab' fragment (<sup>99m</sup>Tc-DI-DD3B6/22-80B3): Results of a phase I trial. *Eur J Nucl Med Mol Imaging*. 2009; 36:250–9. [PubMed: 18800218]

35. Morris TA, Gerometta M, Smart RC, Eisenberg P, Roach PJ, Tsui WW, et al. Pulmonary emboli imaging with  $^{99m}\text{Tc}$ -labelled anti-D-dimer (DI-80B3) Fab' followed by SPECT. *Heart Lung Circ.* 2011; 20:503–11. [PubMed: 21570351]
36. Perrier A, Desmarais S, Goehring C, de Moerloose P, Morabia A, Unger PF, et al. D-dimer testing for suspected pulmonary embolism in outpatients. *Am J Respir Crit Care Med.* 1997; 156:492–6. [PubMed: 9279229]
37. Smith GP. Filamentous fusion phage: Novel expression vectors that display cloned antigens on the virion surface. *Science.* 1985; 228:1315–7. [PubMed: 4001944]
38. Overoye-Chan K, Koerner S, Looby RJ, Kolodziej AF, Zech SG, Deng Q, et al. EP-2104R: A fibrin-specific gadolinium-based MRI contrast agent for detection of thrombus. *J Am Chem Soc.* 2008; 130:6025–39. [PubMed: 18393503]
39. Kolodziej AF, Nair SA, Graham P, McMurry TJ, Ladner RC, Wescott C, et al. Fibrin specific peptides derived by phage display: Characterization of peptides and conjugates for imaging. *Bioconjug Chem.* 2012; 23:548–56. [PubMed: 22263840]
40. Botnar RM, Buecker A, Wiethoff AJ, Parsons EC Jr, Katoh M, Katsimaglis G, et al. In vivo magnetic resonance imaging of coronary thrombosis using a fibrin-binding molecular magnetic resonance contrast agent. *Circulation.* 2004; 110:1463–6. [PubMed: 15238457]
41. Spuentrup E, Buecker A, Katoh M, Wiethoff AJ, Parsons EC Jr, Botnar RM, et al. Molecular magnetic resonance imaging of coronary thrombosis and pulmonary emboli with a novel fibrin-targeted contrast agent. *Circulation.* 2005; 111:1377–82. [PubMed: 15738354]
42. Spuentrup E, Katoh M, Wiethoff AJ, Parsons EC Jr, Botnar RM, Mahnken AH, et al. Molecular magnetic resonance imaging of pulmonary emboli with a fibrin-specific contrast agent. *Am J Respir Crit Care Med.* 2005; 172:494–500. [PubMed: 15937292]
43. Spuentrup E, Fausten B, Kinzel S, Wiethoff AJ, Botnar RM, Graham PB, et al. Molecular magnetic resonance imaging of atrial clots in a swine model. *Circulation.* 2005; 112:396–9. [PubMed: 16009790]
44. Spuentrup E, Botnar RM. Coronary magnetic resonance imaging: visualization of the vessel lumen and the vessel wall and molecular imaging of arteriothrombosis. *Eur Radiol.* 2006; 16:1–14. [PubMed: 16132919]
45. Botnar RM, Perez AS, Witte S, Wiethoff AJ, Laredo J, Hamilton J, et al. In vivo molecular imaging of acute and subacute thrombosis using a fibrin-binding magnetic resonance imaging contrast agent. *Circulation.* 2004; 109:2023–9. [PubMed: 15066940]
46. Sirol M, Fuster V, Badimon JJ, Fallon JT, Moreno PR, Toussaint JF, et al. Chronic thrombus detection with in vivo magnetic resonance imaging and a fibrin-targeted contrast agent. *Circulation.* 2005; 112:1594–600. [PubMed: 16145001]
47. Spuentrup E, Katoh M, Buecker A, Fausten B, Wiethoff AJ, Wildberger JE, et al. Molecular MR imaging of human thrombi in a swine model of pulmonary embolism using a fibrin-specific contrast agent. *Investig Radiol.* 2007; 42:586–95. [PubMed: 17620942]
48. Spuentrup E, Botnar RM, Wiethoff AJ, Ibrahim T, Kelle S, Katoh M, et al. MR imaging of thrombi using EP-2104R, a fibrin-specific contrast agent: Initial results in patients. *Eur Radiol.* 2008; 18:1995–2005. [PubMed: 18425519]
49. Edwards D, Lewis J, Battle M, Lear R, Farrar G, Barnett DJ, et al.  $^{99m}\text{Tc}$ -NC100668, a new tracer for imaging venous thromboemboli: Pre-clinical biodistribution and incorporation into plasma clots in vivo and in vitro. *Eur J Nucl Med Mol Imaging.* 2006; 33:1258–65. [PubMed: 16804686]
50. Edwards D, Lewis J, Battle M, Lear R, Farrar G, Barnett DJ, et al. The biodistribution of NC100668 and the effect of excess NC100668 on the biodistribution and kidney retention of  $^{99m}\text{Tc}$ -NC100668 in the rat. *Nucl Med Biol.* 2007; 34:315–23. [PubMed: 17383581]
51. Edwards D, Lewis J, Battle M, Lear R, Farrar G, Jon Barnett D, et al.  $^{99m}\text{Tc}$ -NC100668, an agent for imaging venous thromboembolism: The effect of anticoagulant or thrombolytic therapy on the uptake and retention of radioactivity in blood clots in vivo. *Nucl Med Commun.* 2007; 28:55–62. [PubMed: 17159550]
52. McIlmoyle G, Davis HH, Welch MJ. Scintigraphic diagnosis of experimental pulmonary embolism with In-111-labeled platelets. *J Nucl Med.* 1977; 18:910–4. [PubMed: 893789]

53. Knight LC, Primeau JL, Siegel BA, Welch MJ. Comparison of In-111-labeled platelets and iodinated fibrinogen for the detection of deep vein thrombosis. *J Nucl Med.* 1978; 19:891–4. [PubMed: 682021]
54. Price DC, Lipton MJ, Lusby RJ, Engelstad BL, Stoney RJ, Prager RJ, et al. In vivo detection of thrombi with indium-111-labeled platelets. *IEEE Trans Nucl Sci.* 1982; 29:1191–7.
55. Fedullo PF, Moser KM, Moser KS, Konopka R, Hartman MT. Indium-111-labeled platelets: Effect of heparin on uptake by venous thrombi and relationship to the activated partial thromboplastin time. *Circulation.* 1982; 66:632–7. [PubMed: 7094273]
56. Stratton JR, Ritchie JL. The effects of antithrombotic drugs in patients with left ventricular thrombi: Assessment with indium-111 platelet imaging and two-dimensional echocardiography. *Circulation.* 1984; 69:561–8. [PubMed: 6692517]
57. Ezekowitz MD, Leonard JC, Smith EO, Allen EW, Taylor FB. Identification of left ventricular thrombi in man using Indium-111-labeled autologous platelets. A preliminary report. *Circulation.* 1981; 63:803–10. [PubMed: 7471335]
58. Vandenberg BF, Seabold JE, Schroder E, Kerber RE. Noninvasive imaging of left ventricular thrombi: Two-dimensional echocardiography and indium-111 platelet scintigraphy. *Am J Card Imaging.* 1987; 1:289–94.
59. Tsuda T, Kubota M, Iwakubo A, Akiba H, Shido M, Takahashi T, et al. Availability of <sup>111</sup>In-labeled platelet scintigraphy in patients with postinfarction left ventricular aneurysm. *Ann Nucl Med.* 1989; 3:15–24. [PubMed: 2518223]
60. Stratton JR, Ritchie JL. <sup>111</sup>In platelet imaging of left ventricular thrombi: Predictive value for systemic emboli. *Circulation.* 1990; 81:1182–9. [PubMed: 2317901]
61. Zoppo GJ, Copeland BR, Harker LA, Waltz TA, Zyroff J, Hanson SR, et al. Experimental acute thrombotic stroke in baboons. *Stroke.* 1986; 17:1254–65. [PubMed: 3810730]
62. Hanson SR, Paxton LD, Harker LA. Iliac artery mural thrombus formation. Effect of antiplatelet therapy on <sup>111</sup>In-platelet deposition in baboons. *Arteriosclerosis.* 1986; 6:511–8. [PubMed: 3767696]
63. Siegel RS, Rae JL, Ryan NL, Edwards C, Fortune WP, Lewis RJ, et al. The use of indium-111 labeled platelet scanning for the detection of asymptomatic deep venous thrombosis in a high risk population. *Orthopedics.* 1989; 12:1439–43. [PubMed: 2685788]
64. Oster ZH, Srivastava SC, Som P, Meinken GE, Scudder LE, Yamamoto K, et al. Thrombus radioimmunoscintigraphy: An approach using monoclonal antiplatelet antibody. *Proc Natl Acad Sci USA.* 1985; 82:3465–8. [PubMed: 3858832]
65. Gu J, Liu Y, Xia L, Wan H, Li P, Zhang X, et al. Construction and expression of mouse-human chimeric antibody SZ-51 specific for activated platelet P-selectin. *Thromb Haemost.* 1997; 77:755–9. [PubMed: 9134655]
66. Wu G. Application of a monoclonal antibody SZ-51 specific for activated human platelets in canine thrombosis imaging. *Zhonghua yi xue za zhi.* 1991; 71:605–7. 42. [PubMed: 1725498]
67. Gu JM, Liu Y, Wan HY, Li PX, Ruan CG. Construction and expression of mouse-human chimeric antibody SZ-51 specific for human activated platelets. *Acta Biochim Biophys Sin.* 1996; 28:469–70.
68. Mousa SA, Bozarth JM, Edwards S, Carroll T, Barrett J. Novel technetium-99m-labeled platelet GPIIb/IIIa receptor antagonists as potential imaging agents for venous and arterial thrombosis. *Coron Artery Dis.* 1998; 9:131–41. [PubMed: 9647415]
69. Edwards DS, Liu S, Barrett JA, Harris AR, Looby RJ, Ziegler MC, et al. New and versatile ternary ligand system for tech-netium radiopharmaceuticals: Water soluble phosphines and tricine as coligands in labeling a hydrazinonicotinamide-modified cyclic glycoprotein IIb/IIIa receptor antagonist with <sup>99m</sup>Tc. *Bioconjug Chem.* 1997; 8:146–54. [PubMed: 9095354]
70. Barrett JA, Dampousse DJ, Heminway SJ, Liu S, Scott Edwards D, Looby RJ, et al. Biological evaluation of <sup>99m</sup>Tc-labeled cyclic glycoprotein IIb/IIIa receptor antagonists in the canine arteriovenous shunt and deep vein thrombosis models: Effects of chelators on biological properties of <sup>99m</sup>Tc chelator-peptide conjugates. *Bioconjug Chem.* 1996; 7:203–8. [PubMed: 8983342]



71. Knight LC, Romano JE, Maurer AH. In vitro platelet binding compared with in vivo thrombus imaging using  $\alpha$ (IIb) $\beta$ 3-targeted radioligands. *Thromb Haemost*. 1998; 80:845–51. [PubMed: 9843182]
72. Knight LC, Baidoo KE, Romano JE, Gabriel JL, Maurer AH. Imaging pulmonary emboli and deep venous thrombi  $^{99m}\text{Tc}$ -bitistatin, a platelet-binding polypeptide from viper venom. *J Nucl Med*. 2000; 41:1056–64. [PubMed: 10855635]
73. Baidoo KE, Knight LC, Lin KS, Gabriel JL, Romano JE. Design and synthesis of a short-chain bitistatin analogue for imaging thrombi and emboli. *Bioconjug Chem*. 2004; 15:1068–75. [PubMed: 15366961]
74. Mitchel J, Waters D, Lai T, White M, Alberghini T, Salloum A, et al. Identification of coronary thrombus with a IIb/IIIa platelet inhibitor radiopharmaceutical, technetium-99m DMP-444: A canine model. *Circulation*. 2000; 101:1643–6. [PubMed: 10758044]
75. Taillefer R, Edell S, Innes G, Lister-James J. Multicenter Trial Investigators. Acute thromboscintigraphy with  $^{99m}\text{Tc}$ -apcptide: results of the phase 3 multicenter clinical trial comparing  $^{99m}\text{Tc}$ -apcptide scintigraphy with contrast venography for imaging acute DVT. *J Nucl Med*. 2000; 41:1214–23. [PubMed: 10914912]
76. Scharn DM, Oyen WJG, Klemm PL, Wijnen MHWA, VanderVliet JA. Assessment of prosthetic vascular graft thrombogenicity using the technetium-99m labeled glycoprotein IIb/IIIa receptor antagonist DMP444 in a dog model. *Vascular*. 2002; 10:566–9.
77. Tung CH, Quinti L, Jaffer FA, Weissleder R. A branched fluorescent peptide probe for imaging of activated platelets. *Mol Pharm*. 2005; 2:92–5. [PubMed: 15804182]
78. Klink A, Lancelot E, Ballet S, Vucic E, Fabre JE, Gonzalez W, et al. Magnetic resonance molecular imaging of thrombosis in an arachidonic acid mouse model using an activated platelet targeted probe. *Arterioscler Thromb Vasc Biol*. 2010; 30:403–10. [PubMed: 20139362]
79. Lanza G, Wallace K, Scott M, Cacheris W, Abendschein D, Christy D, et al. A novel site-targeted ultrasonic contrast agent with broad biomedical application. *Circulation*. 1996; 94:3334–40. [PubMed: 8989148]
80. Lanza GM, Wallace KD, Fischer SE, Christy DH, Scott MJ, Trousil RL, et al. High-frequency ultrasonic detection of thrombi with a targeted contrast system. *Ultrasound Med Biol*. 1997; 23:863–70. [PubMed: 9300990]
81. Lanza G, Trousil R, Wallace K, Rose J, Hall C, Scott M, et al. In vitro characterization of a novel, tissue-targeted ultrasonic contrast system with acoustic microscopy. *J Acoust Soc Am*. 1998; 104:3665–72. [PubMed: 9857523]
82. Hughes MS, Marsh JN, Hall CS, Fuhrhop RW, Lacy EK, Lanza GM, et al. Acoustic characterization in whole blood and plasma of site-targeted nanoparticle ultrasound contrast agent for molecular imaging. *J Acoust Soc Am*. 2005; 117:964–72. [PubMed: 15759715]
83. Hughes MS, Marsh JN, Hall CS, Savery D, Lanza GM, Wickline SA. Characterization of digital waveforms using thermodynamic analogs: Applications to detection of materials defects. *IEEE Trans Ultrasonics Ferroelectr Freq Control*. 2005; 52:1555–64.
84. Hughes MS, Marsh JN, Zhang H, Woodson AK, Allen JS, Lacy EK, et al. Characterization of digital waveforms using thermodynamic analogs: Detection of contrast-targeted tissue in vivo. *IEEE Trans Ultrasonics Ferroelectr Freq Control*. 2006; 53:1609–16.
85. Hughes MS, McCarthy JE, Marsh JN, Arbeit JM, Neumann RG, Fuhrhop RW, et al. Properties of an entropy-based signal receiver with an application to ultrasonic molecular imaging. *J Acoust Soc Am*. 2007; 121:3542–57. [PubMed: 17552706]
86. Hughes MS, Marsh JN, Arbeit JM, Neumann RG, Fuhrhop RW, Wallace KD, et al. Application of Renyi entropy for ultrasonic molecular imaging. *J Acoust Soc Am*. 2009; 125:3141–5. [PubMed: 19425656]
87. Alkan-Onyuksel H, Demos S, Lanza G, Vonesh M, Klegerman M, Kane B, et al. Development of inherently echogenic liposomes as an ultrasonic contrast agent. *J Pharm Sci*. 1996; 85:486–90. [PubMed: 8742939]
88. Demos S, Onyuksel H, Gilbert J, Roth S, Kane B, Jungblut P, et al. In vitro targeting of antibody-conjugated echogenic liposomes for site-specific ultrasonic image enhancement. *J Pharm Sci*. 1997; 86:161–71.



89. Demos S, Alkan-Onyuksel H, Kane B, Ramani K, Nagaraj A, Greene R, et al. In vivo targeting of acoustically reflective liposomes for intravascular and transvascular ultrasonic enhancement. *J Am Coll Cardiol.* 1999; 33:867–75. [PubMed: 10080492]
90. Tiukinhoy-Laing SD, Huang S, Klegerman M, Holland CK, McPherson DD. Ultrasound-facilitated thrombolysis using tissue-plasminogen activator-loaded echogenic liposomes. *Thromb Res.* 2007; 119:777–84. [PubMed: 16887172]
91. Huang SL, Kee PH, Kim H, Moody MR, Chrzanowski SM, Macdonald RC, et al. Nitric oxide-loaded echogenic liposomes for nitric oxide delivery and inhibition of intimal hyperplasia. *J Am Coll Cardiol.* 2009; 54:652–9. [PubMed: 19660697]
92. Shaw GJ, Meunier JM, Huang SL, Lindsell CJ, McPherson DD, Holland CK. Ultrasound-enhanced thrombolysis with tPA-loaded echogenic liposomes. *Thromb Res.* 2009; 124:306–10. [PubMed: 19217651]
93. Britton GL, Kim H, Kee PH, Aronowski J, Holland CK, McPherson DD, et al. In vivo therapeutic gas delivery for neuroprotection with echogenic liposomes. *Circulation.* 2010; 122:1578–87. [PubMed: 20921443]
94. Kim H, Britton GL, Peng T, Holland CK, McPherson DD, Huang SL. Nitric oxide-loaded echogenic liposomes for treatment of vasospasm following subarachnoid hemorrhage. *Int J Nanomed.* 2014; 9:155–65.
95. Alonso A, Martina AD, Stroick M, Fatar M, Griebel M, Pochon S, et al. Molecular imaging of human thrombus with novel abciximab immunobubbles and ultrasound. *Stroke.* 2007; 38:1508–14. [PubMed: 17379828]
96. Savitha, F; Forsberg, F; Gilmore, SC; Shevchuk, SV; Kerschen, A; Matsunaga, TO; , et al. Adherence of platelet and fibrin targeted ultrasound contrast bubbles to human blood clots in vitro. 2008 IEEE International Ultrasonics Symposium; 2008; 349–52.
97. Wang X, Hagemeyer CE, Hohmann JD, Leitner E, Armstrong PC, Jia F, et al. Novel single-chain antibody-targeted microbubbles for molecular ultrasound imaging of thrombosis: Validation of a unique noninvasive method for rapid and sensitive detection of thrombi and monitoring of success or failure of thrombolysis in mice. *Circulation.* 2012; 125:3117–26. [PubMed: 22647975]
98. Hu G, Liu C, Liao Y, Yang L, Huang R, Wu J, et al. Ultrasound molecular imaging of arterial thrombi with novel microbubbles modified by cyclic RGD in vitro and in vivo. *Thromb Haemost.* 2012; 107:172–83. [PubMed: 22116307]
99. Wu W, Wang Y, Shen S, Wu J, Guo S, Su L, et al. In vivo ultrasound molecular imaging of inflammatory thrombosis in arteries with cyclic Arg-Gly-Asp-modified microbubbles targeted to glycoprotein IIb/IIIa. *Investig Radiol.* 2013; 48:803–12. [PubMed: 23857134]
100. Hua X, Liu P, Gao YH, Tan KB, Zhou LN, Liu Z, et al. Construction of thrombus-targeted microbubbles carrying tissue plasminogen activator and their in vitro thrombolysis efficacy: A primary research. *J Thromb Thrombolysis.* 2010; 30:29–35. [PubMed: 20155435]
101. Wang X, Gkanatsas Y, Palasubramaniam J, Hohmann JD, Chen YC, Lim B, et al. Thrombus-targeted theranostic microbubbles: A new technology towards concurrent rapid ultrasound diagnosis and bleeding-free fibrinolytic treatment of thrombosis. *Theranostics.* 2016; 6:726–38. [PubMed: 27022419]
102. Lanza GM, Lorenz CH, Fischer SE, Scott MJ, Cacheris WP, Kaufmann RJ, et al. Enhanced detection of thrombi with a novel fibrin-targeted magnetic resonance imaging agent. *Acad Radiol.* 1998; 5:S173–6. [PubMed: 9561074]
103. Winter P, Caruthers S, Yu X, Song S, Fuhrhop R, Chen J, et al. Improved molecular imaging contrast agent for detection of human thrombus. *Magn Reson Med.* 2003; 50:411–6. [PubMed: 12876719]
104. Pham CT, Mitchell LM, Huang JL, Lubniewski CM, Schall OF, Killgore JK, et al. Variable antibody-dependent activation of complement by functionalized phospholipid nanoparticle surfaces. *J Biol Chem.* 2011; 286:123–30. [PubMed: 21047788]
105. Temme S, Grapentin C, Quast C, Jacoby C, Grandoch M, Ding Z, et al. Noninvasive imaging of early venous thrombosis by <sup>19</sup>F magnetic resonance imaging with targeted perfluorocarbon nanoemulsions. *Circulation.* 2015; 131:1405–14. [PubMed: 25700177]

106. Yu X, Song S-K, Chen J, Scott M, Fuhrhop R, Hall C, et al. High-resolution MRI characterization of human thrombus using a novel fibrin-targeted paramagnetic nanoparticle contrast agent. *Magn Reson Med*. 2000; 44:867–72. [PubMed: 11108623]
107. Flacke S, Fischer S, Scott M, Fuhrhop R, Allen J, Mc Lean M, et al. A novel MRI contrast agent for molecular imaging of fibrin: implications for detecting vulnerable plaques. *Circulation*. 2001; 104:1280–5. [PubMed: 11551880]
108. Johansson LO, Bjornerud A, Ahlstrom HK, Ladd DL, Fujii DK. A targeted contrast agent for magnetic resonance imaging of thrombus: Implications of spatial resolution. *J Magn Reson Imaging*. 2001; 13:615–8. [PubMed: 11276107]
109. von zur Muhlen C, von Elverfeldt D, Moeller JA, Choudhury RP, Paul D, Hagemeyer CE, et al. Magnetic resonance imaging contrast agent targeted toward activated platelets allows in vivo detection of thrombosis and monitoring of thrombolysis. *Circulation*. 2008; 118:258–67. [PubMed: 18574047]
110. Gleich B, Weizenecker J. Tomographic imaging using the nonlinear response of magnetic particles. *Nature*. 2005; 435:1214–7. [PubMed: 15988521]
111. Starmans LWE, Burdinski D, Haex NPM, Moonen RPM, Strijkers GJ, Nicolay K, et al. Iron oxide nanoparticle-micelles (ION-Micelles) for sensitive (Molecular) magnetic particle imaging and magnetic resonance imaging. *PLoS ONE*. 2013; 8:e57335. [PubMed: 23437371]
112. Phinikaridou A, Andia ME, Saha P, Modarai B, Smith A, Botnar RM. In vivo magnetization transfer and diffusion-weighted magnetic resonance imaging detects thrombus composition in a mouse model of deep vein thrombosis. *Circ Cardiovasc Imaging*. 2013; 6:433–40. [PubMed: 23564561]
113. Myerson J, He L, Lanza G, Tollefsen D, Wickline S. Thrombin-inhibiting perfluorocarbon nanoparticles provide a novel strategy for the treatment and magnetic resonance imaging of acute thrombosis. *J Thromb Haemost*. 2011; 9:1292–300. [PubMed: 21605330]
114. Winter PM, Shukla HP, Caruthers SD, Scott MJ, Fuhrhop RW, Robertson JD, et al. Molecular imaging of human thrombus with computed tomography. *Acad Radiol*. 2005; 12:S9–13. [PubMed: 16106538]
115. Mattrey RF, Scheible FW, Gosink BB, Leopold GR, Long DM, Higgins CB. Perfluorooctylbromide: a liver/spleen-specific and tumor-imaging ultrasound contrast material. *Radiology*. 1982; 145:759–62. [PubMed: 7146409]
116. Sartoris DJ, Guerra J Jr, Mattrey RF, Resnick D, Haghighi P, Mitten R, et al. Perfluorooctylbromide as a contrast agent for computed tomographic imaging of septic and aseptic arthritis. *Investig Radiol*. 1986; 21:49–55. [PubMed: 3943957]
117. Mattrey RF, Hajek PC, Gylys-Morin VM, Baker LL, Martin J, Long DC, et al. Perfluorochemicals as gastrointestinal contrast agents for MR imaging: Preliminary studies in rats and humans. *AJR Am J Roentgenol*. 1987; 148:1259–63. [PubMed: 3495156]
118. Schirra CO, Brendel B, Anastasio MA, Roessl E. Spectral CT: A technology primer for contrast agent development. *Contrast Media Mol Imaging*. 2014; 9:62–70. [PubMed: 24470295]
119. Pan D, Roessl E, Schlomka JP, Caruthers SD, Senpan A, Scott MJ, et al. Computed tomography in color: NanoK-enhanced spectral CT molecular imaging. *Angew Chem Int Ed Engl*. 2010; 49:9635–9. [PubMed: 21077082]
120. Pan D, Schirra CO, Senpan A, Schmieder AH, Stacy AJ, Roessl E, et al. An early investigation of ytterbium nanocolloids for selective and quantitative “multicolor” spectral CT imaging. *ACS Nano*. 2012; 6:3364–70. [PubMed: 22385324]
121. Schirra CO, Senpan A, Roessl E, Thran A, Stacy AJ, Wu L, et al. Second generation gold nanobeacons for robust K-edge imaging with multi-energy CT. *J Mater Chem*. 2012; 22:23071–7. [PubMed: 23185109]
122. Pan D, Schirra CO, Wickline SA, Lanza GM. Multicolor computed tomographic molecular imaging with noncrystalline high-metal-density nanobeacons. *Contrast Media Mol Imaging*. 2014; 9:13–25. [PubMed: 24470291]
123. Chrastina A, Valadon P, Massey KA, Schnitzer JE. Lung vascular targeting using antibody to aminopeptidase P: CT-SPECT imaging, biodistribution and pharmacokinetic analysis. *J Vasc Res*. 2010; 47:531–43. [PubMed: 20431301]

124. Clausen DM, Guo J, Parise RA, Beumer JH, Egorin MJ, Lazo JS, et al. In vitro cytotoxicity and in vivo efficacy, pharmacokinetics, and metabolism of 10074-G5, a novel small-molecule inhibitor of c-Myc/Max dimerization. *J Pharmacol Exp Ther*. 2010; 335:715–27. [PubMed: 20801893]
125. Conti G, Tambalo S, Villetti G, Catinella S, Carnini C, Bassani F, et al. Evaluation of lung inflammation induced by intratracheal administration of LPS in mice: Comparison between MRI and histology. *Magn Reson Mater Phys Biol Med*. 2010; 23:93–101.
126. Cormode DP, Roessl E, Thran A, Skajaa T, Gordon RE, Schlomka J-P, et al. Atherosclerotic plaque composition: analysis with multicolor CT and targeted gold nanoparticles. *Radiology*. 2010; 256:774–82. [PubMed: 20668118]
127. Jaffer FA, Tung CH, Wykrzykowska JJ, Ho NH, Houg AK, Reed GL, et al. Molecular imaging of factor XIIIa activity in thrombosis using a novel, near-infrared fluorescent contrast agent that covalently links to thrombi. *Circulation*. 2004; 110:170–6. [PubMed: 15210587]
128. Hara T, Bhayana B, Thompson B, Kessinger CW, Khatri A, McCarthy JR, et al. Molecular imaging of fibrin deposition in deep vein thrombosis using fibrin-targeted near-infrared fluorescence. *JACC*. 2012; 5:607–15. [PubMed: 22698530]
129. Stein-Merlob AF, Kessinger CW, Sibel Erdem S, Zelada H, Hilderbrand SA, Lin CP, et al. Blood accessibility to fibrin in venous thrombosis is thrombus age-dependent and predicts fibrinolytic efficacy: An in vivo fibrin molecular imaging study. *Theranostics*. 2015; 5:1317–27. [PubMed: 26516370]
130. Pan D, Pramanik M, Senpan A, Yang X, Song KH, Scott MJ, et al. Molecular photoacoustic tomography with colloidal nanobeacons. *Angew Chem Int Ed Engl*. 2009; 48:4170–3. [PubMed: 19418503]
131. Pan D, Caruthers SD, Senpan A, Yalaz C, Stacy AJ, Hu G, et al. Synthesis of NanoQ, a copper-based contrast agent for high-resolution magnetic resonance imaging characterization of human thrombus. *J Am Chem Soc*. 2011; 133:9168–71. [PubMed: 21599030]
132. Zhang R, Pan D, Cai X, Yang X, Senpan A, Allen JS, et al. Alpha nu beta 3-targeted copper nanoparticles incorporating an Sn 2 lipase-labile fumagillin prodrug for photoacoustic neovascular imaging and treatment. *Theranostics*. 2015; 5:124–33. [PubMed: 25553103]
133. Ciesinski KL, Yang Y, Ay I, Chonde DB, Loving GS, Rietz TA, et al. Fibrin-targeted PET probes for the detection of thrombi. *Mol Pharm*. 2013; 10:1100–10. [PubMed: 23327109]
134. Blasi F, Oliveira BL, Rietz TA, Rotile NJ, Day H, Naha PC, et al. Radiation dosimetry of the fibrin-binding probe <sup>64</sup>Cu-FBP8 and Its feasibility for PET imaging of deep vein thrombosis and pulmonary embolism in rats. *J Nucl Med*. 2015; 56:1088–93. [PubMed: 25977464]
135. Blasi F, Oliveira BL, Rietz TA, Rotile NJ, Naha PC, Cormode DP, et al. Multisite thrombus imaging and fibrin content estimation with a single whole-body PET scan in rats. *Arterioscler Thromb Vasc Biol*. 2015; 35:2114–21. [PubMed: 26272938]

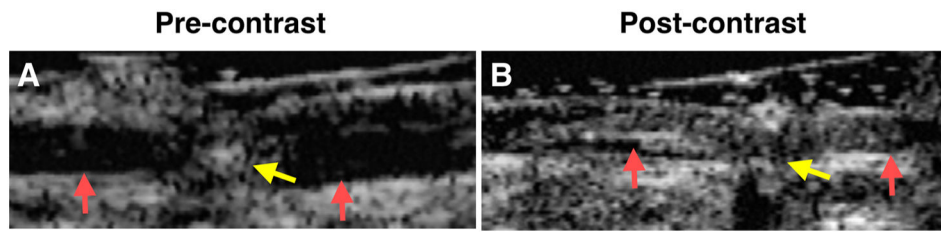


**Figure 1.** Acoustic enhancement of canine femoral artery thrombus, targeted with biotinylated anti-fibrin antibody, before (**A**) and after (**B**) exposure to targeted perfluorocarbon emulsion. Pre-contrast the acute arterial thrombus is poorly visualized with a 7.5-MHz linear-array, focused transducer. The transmural electrode (*yellow arrow*) and the wall boundaries of the femoral artery are clearly delineated. Post contrast the thrombus is easily recognized (*red arrows before and after*) exposure. Reproduced with permission Reference.<sup>79</sup>

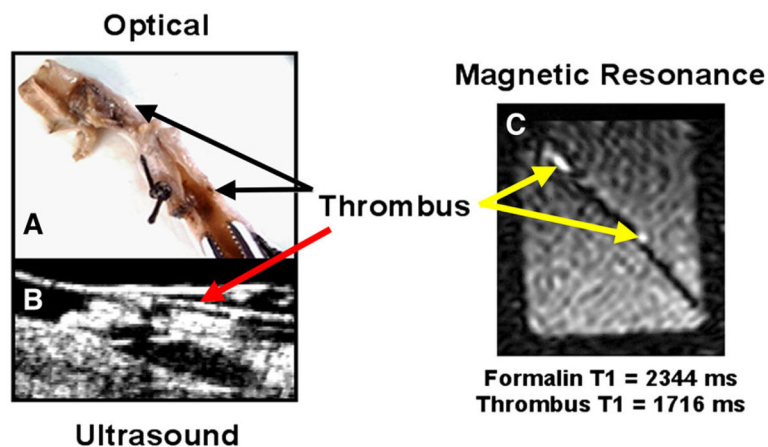


**Figure 2.**

**A** White light image of canine femoral artery with recovered segmented thrombus, following recovery, formed as described in Figure 1 with electrical current to draw platelets toward anodal needle tip to propagate clot. **B** Ultrasound imaging obtained in vivo in the canine femoral artery prior to excision showing thrombus. **C** Ex vivo T1-weighted MRI image (1.5T) of excised artery in beaker of buffer. These data present the first demonstration of in vivo targeting of thrombus with a dual modality US–MR perfluorocarbon nanoparticle in canines showing close correspondence between the light, ultrasound, and MR images.<sup>102</sup>

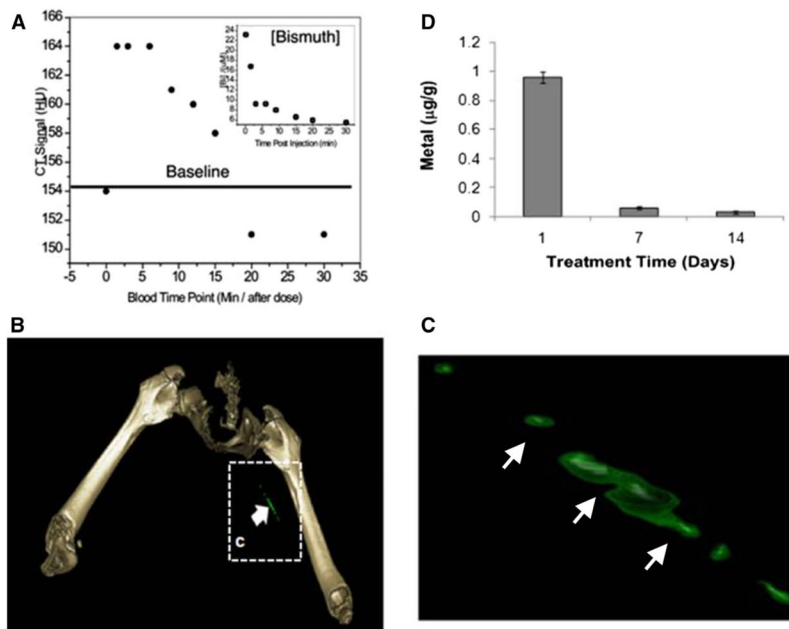


**Figure 3.** (A) CT blood pool signal in rabbits following IV injection of NanoK. CT scan imaging parameters were thickness 0.8, increment 0.8, kV 90, mAs 1500, resolution HIGH, collimation  $4 \times 0.75$ , pitch 0.35, rotation time 1.5 seconds, FOV 75 mm. *Inset* The concentration of bismuth (ICP) in blood vs time post-injection. Note that the background signal is at baseline in less than 30 minutes; (B, C) targeting in situ clot (thrombus) in rabbits; (D) 2 weeks clearance profile of bismuth from mice. Reproduced with permission. 119